N.F. Morrison and O.G. Harlen, in Proc 27th Int. Conf. on Digital Printing Technologies, NIP27, Minneapolis, MN, USA, 2011, 360-364, 'Inkjet printing of non-Newtonian fluids'.

Inkjet printing of non-Newtonian fluids

Neil F. Morrison and Oliver G. Harlen; Department of Applied Mathematics; University of Leeds, Leeds, LS2 9JT, U.K.

Abstract

Jet breakup is strongly affected by fluid rheology. In particular, small amounts of polymer can cause substantially different breakup dynamics compared to a Newtonian jet, influencing in-flight fragmentation and detachment from the nozzle. Significant concentrations may also impede jettability. Furthermore, most commercial and industrial inks are inherently colloidal due to the presence of pigment and other additives. Fluids containing a particulate phase are normally shear-thinning and so may have a different characteristic viscosity within the nozzle compared to the ejected ligament. We have developed numerical simulations using a Lagrangian finite element method that captures the free surface automatically, and admits a variety of viscosity dependences, e.g. on the local shear rate (generalized Newtonian fluid) or on the particle concentration (Krieger-Dougherty type models), in addition to several viscoelastic models for polymeric fluids. This method has been benchmarked against experimental data for Newtonian jets. Appropriate rheological models are discussed, and results are presented alongside comparisons with experimental work.

Introduction

Among the major challenges in contemporary inkjet research are the enhancements of the speed, resolution, and material diversity of the process in order to broaden the range of industrial and commercial applications. These challenges may be addressed in a number of ways depending on the extent to which each constituent part of the process may be modified, for example, by changing the nozzle shape or the drive waveform, or by adjusting the (Newtonian) fluid properties of the ink. Another approach is to exploit non-Newtonian fluid effects, and this has led to several new applications of inkjet technology [1]; viscoelasticity can profoundly influence jetting behaviour [2] [3], as can the presence of a particulate phase [4] [5].

In a drop-on-demand (DOD) inkjet printer, each drop is formed by ejecting an individual ligament of ink from a nozzle; the ligament subsequently either disintegrates into a large main drop and a series of smaller 'satellite' drops, or, preferably, contracts to form a single drop, before impacting on the printing substrate. The fate of the ligament depends on the speed of printing and on the ink viscosity and surface tension (i.e. the Reynolds, Weber, and Ohnesorge numbers of the flow) which control its rate of thinning [6].

Experimental studies of DOD printing are challenging due to the small scales and high speeds involved (a typical nozzle size is 50 μm in diameter with drop speeds of $5\,\mathrm{m\,s^{-1}}$ or above) and the inaccessibility of the flow within the printhead. Recent work has concentrated on controlling ligament lengths and satellite formation [7] [8] [9], reducing drop size [10], and emulating the flow with larger-scale apparatus [11]. Numerical methods have been used to investigate slow pendant drop formation [12] [13] and industrial-speed jetting [14].

The introduction of a polymeric component, even at a low concentration, may significantly alter the breakup behaviour of a fluid thread [15]. Indeed, capillary thinning flows have been used to provide fluid rheometry [16] and to establish the validity of numerical methods [17]. Elasticity accelerates the growth of the capillary instability, but prolongs the lifespan of a thinning thread [2]; the thread thins at an exponential rate while the polymer stretches [18], before breaking when finite extension is reached [19]. During its thinning phase a viscoelastic thread may develop the 'beads on a string' structure [20]. In DOD jetting a variety of breakup types have been observed depending on the concentration and molecular weight of the polymer [21] [22] [23]; these have been reproduced qualitatively in simulations [24].

Shear-thinning fluids may also exhibit different thinning rates to the purely Newtonian case [25] [26]. Fluids with a particulate phase are generally shear-thinning, and as most inks contain either pigment or other additive particles, their rheological characterization [27] [28] is of great importance in understanding and manipulating their jetting behaviours [29]. The shear rates in the nozzle and the thinning ligament may differ by an order of magnitude, and advantage may be taken of this to optimize the effective viscosity of the ink at each stage. Experiments on pendant drop formation of particle suspensions have shown the potential to reduce satellite numbers [4] [5].

In this work we consider the inverse problem of designing an 'ideal ink' based on common industrial requirements. We use a Lagrangian finite element method to simulate DOD printing of shear-thinning and polymeric fluids with the aim of understanding the influence of rheology and making quantitative improvements in printing quality.

Formulation

The simulations use a Lagrangian finite-element method first developed for the study of creeping flow of dilute polymer solutions [30]. The method has since been extended to inertial flows and has been applied to inkjet printing of Newtonian and viscoelastic fluids [11] [24] [31]; details of the computational algorithms may be found in these references.

The shape of the printhead nozzle used in the simulations is identical to that in reference [24], which may be considered a companion paper to the present work; the dimensions are based on those of a Xaar 126 printhead with a nozzle radius $R = 25\,\mu\mathrm{m}$. At the nozzle inlet a time-dependent velocity boundary condition is imposed in the form of a 'pull/push/pull' drive waveform of approximately 30 μs duration; see [24] for further details. In this work we retain the nozzle shape and the drive waveform as constants throughout, except for an overall amplification of the waveform in order to attain the required drop speed $U = 6\,\mathrm{m\,s^{-1}}$. As a consequence of this amplification, the total volume of ejected ink is not fixed.

For a Newtonian fluid of density ρ, viscosity μ, and surface tension γ we define the Reynolds number $\mathrm{Re} = \rho UR/\mu$, the Weber number $\mathrm{We} = \rho U^2 R/\gamma$, and the Ohnesorge number $\mathrm{Oh} = \mu/\sqrt{\rho\gamma R} = \sqrt{\mathrm{We}}/\mathrm{Re}$; the values of these dimensionless quantities determine the relative importance of competing fluid dynamical effects in the flow. Here we keep density and surface tension constant, with We = 27, and we vary viscosity (hence Re and Oh); typical values are Re = 13 and Oh = 0.40 for a real ink. Alternative choices of scalings can result in different dimensionless groupings [6]. For flows without an externally imposed velocity scale it is common to define a capillary time $t_c = \sqrt{\rho R^3/\gamma}$ as the relevant timescale for inertio-capillary breakup [20]. Our timescale is the ratio of length and velocity scales, $T = R/U$, and this is related to the capillary time by $t_c/T = \sqrt{\mathrm{We}}$.

Gravity is negligible on the lengthscales considered in this study. Drag due to air resistance was also neglected in the simulations, as were temperature variations. We assume that the jet is axisymmetric, so that it may be fully described by a cylindrical coordinate system $\{r,\theta,z\}$ with all flow variables independent of θ. The origin is taken as the centre of the nozzle outlet, and the fluid is initially at rest.

The boundary conditions at the free surface are those of zero shear stress and the pressure jump due to surface curvature,

$$\hat{\mathbf{n}}\cdot\boldsymbol{\sigma}\cdot\hat{\mathbf{t}} = 0\,, \qquad \left[\boldsymbol{\sigma}\cdot\hat{\mathbf{n}}\right]_{\mathrm{air}}^{\mathrm{jet}} = -\frac{1}{\mathrm{We}}\left(\frac{1}{R_1}+\frac{1}{R_2}\right)\hat{\mathbf{n}}\,,$$

where $\boldsymbol{\sigma}$ is the dimensionless stress tensor, $\hat{\mathbf{n}}$ is the unit outward normal to the interface, $\hat{\mathbf{t}}$ is the unit tangent in the rz-plane, and R_1 and R_2 are the principal radii of curvature. External air pressure is neglected. Symmetry conditions on the z-axis are $u_r = 0$ and $\sigma_{rz} = 0$, and conditions of no-slip are applied at the rigid interior printhead boundaries. The contact line between the free surface and the printhead is held pinned at the nozzle edge throughout.

The location of the free surface at each time-step is determined implictly via a kinematic condition. In the simulations this is realized automatically, since the mesh is Lagrangian and the mesh nodes are advected with the local fluid velocity.

Fluid models

The governing equations are the conservation of momentum and mass, given in dimensionless form by

$$\frac{\mathrm{D}\mathbf{u}}{\mathrm{D}t} = \nabla\cdot\boldsymbol{\sigma}\,, \qquad \nabla\cdot\mathbf{u} = 0\,, \tag{1}$$

where t, $\mathbf{u}$, and $\boldsymbol{\sigma}$ are the dimensionless time, fluid velocity, and stress respectively. For a Newtonian ink, the stress tensor is

$$\boldsymbol{\sigma} = -p\mathbf{I} + \frac{2}{\mathrm{Re}}\mathbf{E} = -p\mathbf{I} + \frac{1}{\mathrm{Re}}\left(\nabla\mathbf{u} + (\nabla\mathbf{u})^T\right), \tag{2}$$

where p is pressure and $\mathbf{E}$ is the rate of strain tensor; together Eqs. 1 and 2 are the Navier-Stokes equations.

Viscoelastic fluid models have an additional term in the stress tensor; in this work we consider dilute polymer solutions represented by a single-mode FENE-CR model based on a suspension of dumbbell molecules which react as finitely extensible springs [32]. The dimensionless stress tensor for this fluid is

$$\boldsymbol{\sigma} = -p\mathbf{I} + \frac{1}{(1+c)\mathrm{Re}}(2\mathbf{E} - c\overset{\triangledown}{\mathbf{A}})\,, \tag{3}$$

where $\mathbf{A}$ is a symmetric structure tensor which evolves in time as

$$\overset{\triangledown}{\mathbf{A}} \equiv \frac{\mathrm{D}\mathbf{A}}{\mathrm{D}t} - \mathbf{A}\cdot\nabla\mathbf{u} - (\nabla\mathbf{u})^T\cdot\mathbf{A} = -\frac{1}{\mathrm{Wi}}\left(\frac{L^2}{L^2 - \mathrm{Trace}(\mathbf{A})}\right)(\mathbf{A}-\mathbf{I})\,.$$

Here L is the dumbbell extensibility and Wi is the Weissenberg number, which measures the polymer relaxation time τ against the characteristic flow timescale $T = R/U$, i.e. $\mathrm{Wi} = \tau/T$. In Eq. 3 the viscoelastic parameter c may be interpreted as a measure of the concentration of dumbbell molecules [24]. The viscosity in the Reynolds number is then the steady shear viscosity $\mu = \mu_s(1+c)$, where μ_s is the solvent viscosity. The FENE-CR fluid does not shear-thin.

To investigate shear-thinning effects, we also consider a generalized Newtonian fluid model for which the viscosity depends on the local shear rate $\dot{\gamma} = \sqrt{2\mathbf{E}:\mathbf{E}}$ via a response function η. The stress tensor is

$$\boldsymbol{\sigma} = -p\mathbf{I} + \frac{2}{\mathrm{Re}}\eta(\dot{\gamma})\mathbf{E}\,.$$

In particular we use the Carreau fluid model [33], which describes a smooth transition from a zero shear rate viscosity μ_0 to a limiting infinite shear rate viscosity μ_∞. The response function is:

$$\eta(\dot{\gamma}) = \beta + (1-\beta)\left(1 + (\alpha\dot{\gamma})^2\right)^{(n-1)/2}\,, \tag{4}$$

where $\beta = \mu_\infty/\mu_0$, α is a constant associated with the onset of shear-thinning, and n is an index which determines the degree of shear-thinning in the transition; throughout this work we set $n = 0.3$. The viscosity in the Reynolds number is the zero shear rate viscosity μ_0.

In addition to the models discussed above, we have considered several other viscoelastic fluid models and also a colloidal model with viscosity dependence on local particle concentration (cf. Krieger-Dougherty); results are omitted here for brevity.

Shear-thinning results

As our numerical method has already been validated for Newtonian DOD inkjet flows [11] [14] we omit benchmarking details here and proceed directly to the consideration of non-Newtonian effects. The Carreau function η, as defined in Eq. 4, is graphed in Fig. 1 for six values of α (2.4, 4.1, 7.2, 13, 24, and 72, from right to left respectively) with β fixed at 0.06 and Re = 3.4, Oh = 1.6. Other Carreau fluids with different values of β (i.e. μ_0 and μ_∞) were also considered, but results are not included here.

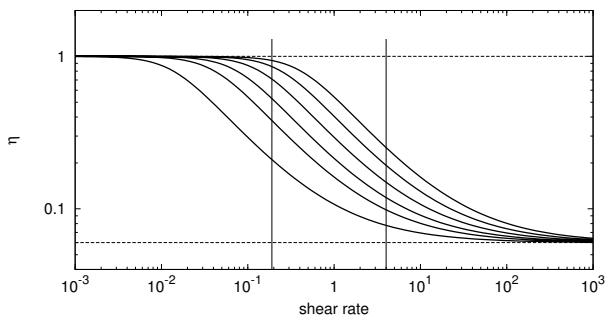

Figure 1. *The Carreau fluid response function $\eta(\dot{\gamma})$ for six values of α.*

The two vertical lines plotted in Fig. 1 represent characteristic values of the dimensionless shear rate during key stages of the flow. The right-hand line ($\dot{\gamma} = 4$) is an approximate maximum rate in the nozzle (achieved during the 'push' phase of the driving), and the left-hand line ($\dot{\gamma} = T/t_c$) is an estimate of the relevant shear rate during the capillary thinning of the ejected ligament. The interval between the two lines corresponds to the range of shear rate variation during the critical stages of ligament ejection and breakup.

Each of the six Carreau fluids was simulated, with the value of the drive amplification factor being calibrated to attain the required drop speed in each case. By comparing these amplification values to those required by Newtonian fluids, we define an effective 'printing viscosity' for each shear-thinning fluid. Results are shown in Fig. 2; the *x*-coordinates of the shear-thinning data points (squares) are Ohnesorge numbers based on these printing viscosities, which may be considered as empirical measures of resistance to jetting.

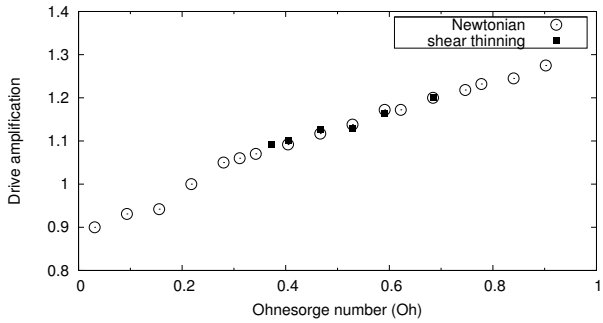

Figure 2. *Drive amplification necessary to attain the required drop speed.*

Amplification factors for a spectrum of Newtonian inks with Ohnesorge numbers between 0 and 1 are shown as circles in Fig. 2. The Newtonian data is roughly linear in Oh apart from a jump after the first four data points (the least viscous fluids); this jump corresponds to a transition in the breakup pattern. In the four least viscous cases the ligament breaks up early into a main drop, a large satellite of comparable volume, and several smaller satellites, whereas in the more viscous cases the large satellite is not formed as the extended ligament lifetime is sufficient for the equivalent part of the fluid to merge with the head of the ligament prior to pinch-off, significantly increasing the volume of the main drop and also slowing it down, so that greater amplification is needed to attain the required printing speed.

The same transition in breakup can also be seen in Fig. 3, which shows the distribution of drop volumes (main drop and major satellites), on a logarithmic scale, for each of the fluids considered. Minor satellite drops with smaller volumes have been ignored in the analysis. As discussed previously, the four least viscous Newtonian cases produce a very large satellite drop, while in the more viscous cases a substantially larger main drop is observed.

It should be noted that for the purposes of this study we did not incorporate any collisions or coalescence of drops after ligament breakup. In some of the simulations it was apparent that such collisions would occur, which could potentially result in minor alterations to the drop volume distributions in Fig. 3. However, our main focus in this work is to consider non-Newtonian effects on the flow dynamics prior to ligament breakup.

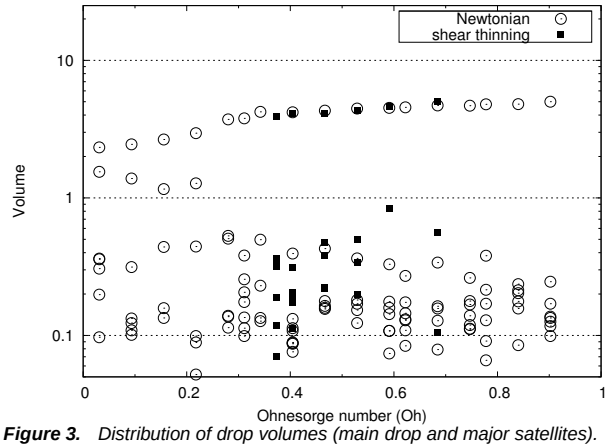

Figure 3. *Distribution of drop volumes (main drop and major satellites).*

Data for the six Carreau fluids are also included in Fig. 3, again using the Ohnesorge numbers based on their effective printing viscosities (as in Fig. 2). For the lower values of Oh, the distribution of drop volumes is similar to the adjacent Newtonian cases. However, for the two largest values of Oh there is a qualitative difference in the breakup pattern: rather than a series of five or six medium-sized satellite drops (as seen in the neighbouring Newtonian cases), we find instead that only one or two significant satellites are formed. In addition the main drop size is increased, but only marginally. The reduction in the number of satellite drops for these cases is not an anomaly; by design, the Carreau fluids exhibit a slower rate of capillary breakup than the nearest Newtonian cases due to their relatively higher viscosity at the shear rates encountered in the ligament thinning phase of the printing, and consequently pinch-off is suppressed and fewer satellites are produced.

The extent to which such a reduction in satellite numbers may be considered an improvement in an industrial context depends on the details of any particular application, but typically it is desirable to suppress the 'quantity' of satellites, both in the discrete sense (as discussed above) and in the continuous sense as follows. For a given printing speed, a simple measure of printing efficiency (or quality) may be defined as the proportion of the total ejected ink which is ultimately contained within the main drop. Although fewer satellites are produced in the more viscous Carreau cases, it is not immediately clear from Fig. 3 whether the efficiency is increased relative to the Newtonian cases because the major Carreau satellite is of greater volume than any of the corresponding Newtonian satellites.

The situation is clarified by Fig. 4: the printing efficiencies of the two most viscous shear-thinning fluids are indeed significantly higher than any of the Newtonian cases. This constitutes a quantitative improvement in printing behaviour, in addition to the qualitative change in satellite distribution. In contrast, the four other Carreau fluids show relatively lower efficiencies, indicating a strong non-Newtonian influence on the printing outcome.

The efficiency for Newtonian fluids initially increases with viscosity before reaching a plateau of around 80%. Again there is a significant jump at around Oh = 0.25, after the first four data points, as a result of the transition in breakup dynamics described

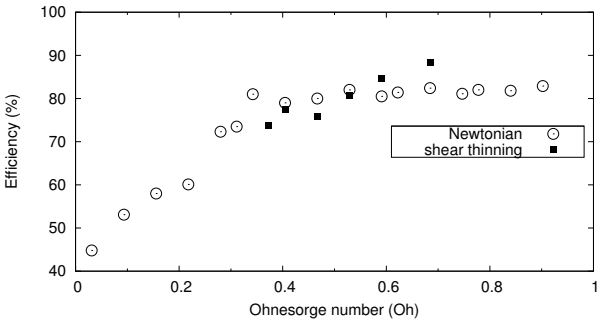

Figure 4. *Efficiency : proportion of total ejected ink within the main drop.*

earlier. It should be emphasized that the results presented here conform to an externally imposed restriction on the speed of the main drop, which is a realistic requirement in many inkjet applications. If this requirement is relaxed, the proportion of ink in the main drop can be increased significantly above the values shown in Fig. 4 even in the Newtonian case, but at the expense of a drastically slower printing speed. However, using the same shear-thinning fluids as described earlier, we have found it possible to achieve up to 100% efficiency at an intermediate printing speed (results not shown here); further exploration of the Carreau model parameter space is ongoing.

Viscoelastic results

Previously our simulations of viscoelastic DOD printing have shown qualitative agreement with jet behaviours observed in experiments [24]. However, no direct correlation was made between the FENE model parameters and the rheological properties of real polymer solutions. Furthermore the jetting speed was not fixed: instead the amplitude of the drive waveform was held constant, meaning that more strongly elastic fluids jetted slower or even retracted into the printhead.

In order to establish quantitative agreement between experiments and simulations of a given fluid at a given printing speed, we apply Zimm theory to linear rheology data obtained via PAV measurements [34] to extract 'best fit' values of the FENE-CR parameters [35]. Details of the Zimm analysis are omitted here for brevity. For two solutions of monodisperse polystyrene (PS210) in diethyl phthalate (DEP) we find $L = 20$ and a relaxation time of around 20 µs (Wi = 4.8), with $c = 0.023$ and $c = 0.046$ for 1000 ppm and 2000 ppm solutions respectively. In Figs. 5 and 6 simulation results (white background) are overlaid on photographs of a real DOD printhead with an array of periodically synchronized nozzles. The close similarity between jet shapes and lengths demonstrates the capacity of both the simulations and the FENE-CR model to quantitatively represent viscoelastic inkjet printing.

Conclusions and future work

Our preliminary investigations have confirmed the potential of shear-thinning effects to positively influence ligament breakup. For some of the cases considered the printing quality was improved in the sense that the overall proportion of ink contained within the main drop was raised significantly, while the number of satellite drops was simultaneously reduced. These improvements were achieved without compromizing on printing speed.

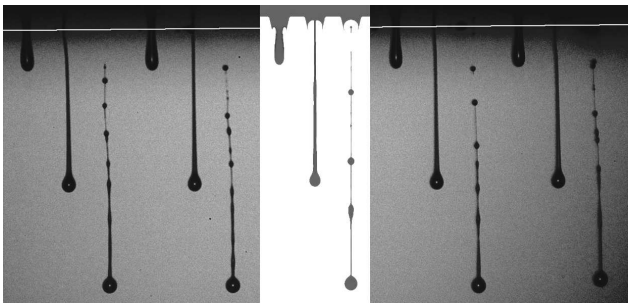

Figure 5. *Comparison for 1000 ppm PS210 in DEP.*

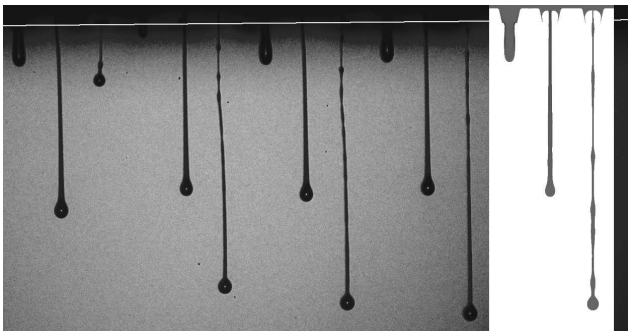

Figure 6. *Comparison for 2000 ppm PS210 in DEP.*

In the cases presented here we have enforced a fixed final drop speed by amplifying the driving waveform appropriately, and consequently the total amount of ejected ink is not a constant of the printing for different fluids. However for some applications it may be more appropriate to impose restrictions on the net ejected volume of ink, or on the volume of the main drop, instead of or in addition to maintaining a consistent drop speed. Further criteria of this nature would necessitate adjustments in the shape of the drive waveform, which could in turn result in qualitative differences in ligament breakup patterns. Such adjustments have not been considered in this work, as the principal aim was to isolate the contribution of non-Newtonian fluid effects.

It remains to be established whether the implications of our findings can be applied directly to the formulation of inks with superior overall printing performance. At present, the Carreau model parameter values used here are not based directly on any real fluid measurements, and there are often practical difficulties associated with the production of an ink designed to adhere to a given theoretical model. In collaboration with industrial and academic experts in the relevant fields, we hope to continue to explore ways of achieving desirable printing consequences by exploiting rheological effects in a manner consistent with the development of real printable inks. In addition we will undertake further investigation of the suitability of other colloidal fluid models.

For viscoelastic fluids we have shown that it is possible to use conventional linear rheology to characterize a given polymeric ink, establish appropriate values of the model parameters, and accurately model its jetting behaviour in simulations. This quantitative validation of our method complements earlier work in which viscoelastic inkjet printing was reproduced qualitatively [24].

Acknowledgments

This work was funded by the U.K. Engineering and Physical Sciences Research Council (EPSRC) and the industrial partners within the Next Generation Inkjet Technology and Innovation in Industrial Inkjet Technology (I4T) projects. The authors are grateful to Steve Hoath for the photographs shown in Figs. 5 and 6, and to Damien Vadillo for data on the linear rheology of the fluids.

References

[1] B.-J. de Gans, P.C. Duineveld, and U.S. Schubert, "*Inkjet printing of polymers: state of the art and future developments*," Adv. Mater., **16** 203 (2004).

[2] M. Goldin, J. Yerushalmi, R. Pfeffer, and R. Shinnar, "*Breakup of a laminar capillary jet of a viscoelastic fluid*," J. Fluid Mech., **38** 689 (1969).

[3] Y. Christanti and L.M. Walker, "*Effect of fluid relaxation time of dilute polymer solutions on jet breakup due to a forced disturbance*," J. Rheol., **46** 733 (2002).

[4] R.J. Furbank and J.F. Morris, "*An experimental study of particle effects on drop formation*," Phys. Fluids, **16** 1777 (2004).

[5] R.J. Furbank and J.F. Morris, "*Pendant drop thread dynamics of particle-laden liquids*," Int. J. Multiphase Flow, **33** 448 (2007).

[6] J. Eggers and E. Villermaux, "*Physics of liquid jets*," Rep. Prog. Phys., **71** 036601 (2008).

[7] H. Dong, W.W. Carr, and J.F. Morris, "*An experimental study of drop-on-demand drop formation*," Phys. Fluids, **18** 072102 (2006).

[8] I.M. Hutchings, G.D. Martin, and S.D. Hoath, "*High speed imaging and analysis of jet and drop formation*," J. Imaging Sci. Technol., **51** 438 (2007).

[9] R. Li, N. Ashgriz, and S. Chandra, "*Droplet generation from pulsed micro-jets*," Exp. Therm. Fluid Sci., **32** 1679 (2008).

[10] A.U. Chen and O.A. Başaran, "*A new method for significantly reducing drop radius without reducing nozzle radius in drop-on-demand drop production*," Phys. Fluids, **14** L1 (2002).

[11] J.R. Castrejón-Pita, N.F. Morrison, O.G. Harlen, G.D. Martin, and I.M. Hutchings, "*Experiments and Lagrangian simulations on the formation of droplets in drop-on-demand mode*," Phys. Rev. E, **83** 036306 (2011).

[12] E.D. Wilkes, S.D. Phillips, and O.A. Başaran, "*Computational and experimental analysis of dynamics of drop formation*," Phys. Fluids, **11** 3577 (1999).

[13] Q. Xu and O.A. Başaran, "*Computational analysis of drop-on-demand drop formation*," Phys. Fluids, **19** 102111 (2007).

[14] S.D. Hoath, G.D. Martin, and I.M. Hutchings, "*Effects of fluid viscosity on drop-on-demand ink-jet break-off*," Proc. NIP26, pg. 10 (2010).

[15] G.H. McKinley, "*Visco-elasto-capillary thinning and breakup of complex fluids*," In Annu. Rheol. Rev. (eds D.M. Binding and K. Walters), British Society of Rheology, **3** 1 (2005).

[16] A.M. Ardekani, V. Sharma, and G.H. McKinley, "*Dynamics of bead formation, filament thinning and breakup in weakly viscoelastic jets*," J. Fluid Mech., **665** 46 (2010).

[17] R. Keunings, "*An algorithm for the simulation of transient viscoelastic flows with free surfaces*," J. Comput. Phys., **62** 199 (1986).

[18] D.W. Bousfield, R. Keunings, G. Marrucci, and M.M. Denn, "*Nonlinear analysis of the surface tension driven breakup of viscoelastic filaments*," J. non-Newtonian Fluid Mech., **21** 79 (1986).

[19] V.M. Entov and E.J. Hinch, "*Effect of a spectrum of relaxation times on the capillary thinning of a filament of elastic liquid*," J. non-Newtonian Fluid Mech., **72** 31 (1997).

[20] C. Clasen, J.Eggers, M.A. Fontelos, J. Li, and G.H. McKinley, "*The beads-on-string structure of viscoelastic threads*", J. Fluid Mech., **556** 283 (2006).

[21] A.V. Bazilevskiy, J.D. Meyer, and A.N. Rozhkov, "*Dynamics and breakup of pulse microjets of polymeric liquids*," Fluid Dynamics, **40** 376 (2005).

[22] H.J. Shore and G.M. Harrison, "*The effect of added polymers on the formation of drops ejected from a nozzle*," Phys. Fluids, **17** 033104 (2005).

[23] S.D. Hoath, G.D. Martin, J.R. Castrejón-Pita, and I.M. Hutchings, "*Satellite formation in drop-on-demand printing of polymer solutions*," Proc. NIP23, pg. 331 (2007).

[24] N.F. Morrison and O.G. Harlen, "*Viscoelasticity in Inkjet Printing*," Rheo. Acta, **49** 619 (2010).

[25] P. Doshi, R. Suryo, Ö.E. Yıldırım, G.H. McKinley, and O.A. Başaran, "*Scaling in pinch-off of generalized Newtonian fluids*," J. non-Newtonian Fluid Mech., **113** 1 (2003).

[26] Ö.E. Yıldırım and O.A. Başaran, "*Deformation and breakup of stretching bridges of Newtonian and shear-thinning liquids: comparison of one- and two-dimensional models*," Chem. Eng. Sci., **56** 211 (2001).

[27] T.R. Tuladhar and M.R. Mackley, "*Filament stretching rheometry and break-up behaviour of low viscosity polymer solutions and inkjet fluids*," J. non-Newtonian Fluid Mech., **148** 97 (2008).

[28] D.C. Vadillo, A.C. Mulji, M.R. Mackley, T.R. Tuladhar, S. Jung, and S.D. Hoath, "*Evaluation of the inkjet fluid's performance using the 'Cambridge Trimaster' filament stretch and break-up device*," J. Rheol., **54** 261 (2010).

[29] S.D. Hoath, I.M. Hutchings, G.D. Martin, T.R. Tuladhar, M.R. Mackley, and D.C. Vadillo, "*Links between ink rheology, drop-on-demand jet formation, and printability*," J. Imaging Sci. Technol., **53** 041208 (2009).

[30] O.G. Harlen, J.M. Rallison, and P. Szabó, "*A split Lagrangian-Eulerian method for simulating transient viscoelastic flows*," J. non-Newtonian Fluid Mech., **60** 81 (1995).

[31] J.R. Castrejón-Pita, N.F. Morrison, O.G. Harlen, G.D. Martin, and I.M. Hutchings, "*Experiments and Lagrangian simulations on the formation of droplets in continuous mode*," Phys. Rev. E, **83** 016301 (2011).

[32] M.D. Chilcott and J.M. Rallison, "*Creeping flow of dilute polymer solutions past cylinders and spheres*," J. non-Newtonian Fluid Mech., **29** 381 (1988).

[33] P.J. Carreau, D. De Kee, and M. Daroux, "*An analysis of the viscous behaviour of polymeric solutions*," Can. J. Chem. Eng., **57** 135 (1979).

[34] D.C. Vadillo, A.C. Mulji, and M.R. Mackley, "*The rheological characterization of linear viscoelasticity for ink jet fluids using piezo axial vibrator and torsion resonator rheometers*," J. Rheol., **54** 781 (2010).

[35] O.G. Harlen, N.F. Morrison, S. Yarlanki, and S.D. Hoath, "*Jet breakup of polymeric fluids in inkjet printing*," IMA Workshop (2009), http://www.ima.umn.edu/2009-2010/W10.12-16.09/

Author Biography

Neil F. Morrison received his MA in mathematics (2007) and his PhD in complex fluid dynamics (2008) from the University of Cambridge. Since then he has worked at the Department of Applied Mathematics at the University of Leeds. His recent research involves the development of computational techniques for the simulation of flows of complex fluids.